ISSN 1063-7834, Physics of the Solid State, 2006, Vol. 48, No. 1, pp. 177–184. © Pleiades Publishing, Inc., 2006.
Original Russian Text © P.V. Avramov, B.I. Yakobson, G.E. Scuseria, 2006, published in Fizika Tverdogo Tela, 2006, Vol. 48, No. 1, pp. 164–171.

FULLERENES AND ATOMIC CLUSTERS

Mechanisms of Inelastic Scattering of Low-Energy Protons by C_6H_6, C_{60}, C_6F_{12}, and $C_{60}F_{48}$ Molecules

P. V. Avramov[1, 2], B. I. Yakobson[2], and G. E. Scuseria[2]

[1] *Kirensky Institute of Physics, Siberian Division, Russian Academy of Sciences, Akademgorodok, Krasnoyarsk, 660036 Russia*

e-mail: avramov.pavel@jaea.go.jp, paul@iph.krasn.ru

[2] *Center for Biological and Environmental Nanotechnology, Rice University, Houston, Texas, 77005-1892 USA*

Received April 25, 2005

Abstract—The mechanisms of inelastic scattering of low-energy protons with a kinetic energy of 2–7 eV by C_6H_6, C_6F_{12}, C_{60}, and $C_{60}F_{48}$ molecules are studied using the methods of quantum chemistry and nonempirical molecular dynamics. It is shown that, for the C_6H_6 + proton and C_{60} + proton systems, starting from a distance of 6 Å from the carbon skeleton, the electronic charge transfer from the aromatic molecule to H^+ occurs with a probability close to unity and transforms the H^+ ion into a hydrogen atom and the neutral C_6H_6 and C_{60} molecules into cation radicals. The mechanism of interaction of low-energy protons with C_6F_{12} and $C_{60}F_{48}$ molecules has a substantially different character and can be considered qualitatively as the interaction between a neutral molecule and a point charge. The Coulomb perturbation of the system arising from the interaction of the noncompensated proton charge with the Mulliken charges of fluorine atoms results in an inversion of the energies of the electronic states localized, on the one hand, on the positively charged hydrogen ion and, on the other hand, on the C_6F_{12} and $C_{60}F_{48}$ molecules. As a result, the neutral molecule + proton state becomes the ground state. In turn, this inversion makes the electronic charge transfer energetically unfavorable. Quantum-chemical and molecular-dynamics calculations on different levels of theory showed that, for fluorine derivatives of some aromatic structures (C_6F_{12}, $C_{60}F_{48}$), the barriers to proton penetration through carbon hexagons are two to four times lower than for the corresponding parent systems (C_6H_6, C_{60}). This effect is explained by the absence of active π-electrons in the case of fluorinated molecules.

PACS numbers: 61.48.+c, 61.80.Lj

DOI: 10.1134/S106378340601032X

1. INTRODUCTION

To date, the development of an effective method of synthesis of endohedral fullerene complexes and nanotubes remains a priority in the chemistry of nanostructures. There are now a number of ways to prepare such nanostructures: (1) high-temperature synthesis in a carbon plasma [1, 2], (2) processing of carbon nanostructures by H_2 and He gases under high pressure [3, 4], (3) irradiation of carbon nanoclusters by ion beams of sufficiently high energies (30–40 eV or more) [5, 6], and (4) radioactive decay of some elements [7].

For the case of irradiation of fullerite by Li^+ ions, the chemical yield of synthesis is about 30% [6], whereas in all other cases the output is much lower (0.1–0.01% or less). The endohedral or exohedral complexes with other atomic species (for example, atoms of alkaline metals) often result in significant changes in the chemical properties and structures of carbon nanoclusters (in particular, due to the formation of various polymers [8] because of the appearance of carbon anion radical forms during metal oxidation by fullerene molecules).

Earlier, the potential barrier to the penetration of a proton into a fullerene molecule was calculated by quantum-chemical PRDDO and DFT methods [9] (3.8 eV) as the difference between the total energies of a neutral $C_{60}H$ molecule (hydrogen covalently bonded to one of the carbon atoms on the external side of the C_{60} molecule) and a neutral transition complex where the proton is at the center of a relaxed carbon hexagon. The potential barriers for a He atom have been calculated by the molecular mechanics method (9.4 eV) [10], semiempirical MNDO method [11] (11.5 eV), or using the second-order Meller–Plesset perturbation theory (MP2) with the 6-31G** basis set [12] (10.7 eV for the C_6H_6 molecule). In [13], molecular-dynamics simulation of the penetration of a Li^+ ion was performed using a DFT potential and it was shown that, for this particle, the barrier height to the penetration into a fullerene polyhedron is below 5 eV.

An immediate reason for the high penetration potential of some ions and atoms through a carbon network and, hence, a low chemical yield of the synthesis can be the electronic π system of carbon nanostructures, which tends to form new covalent bonds at the external side of these objects. Hence, the best way to lower this potential barrier could be to neutralize this system by satura-

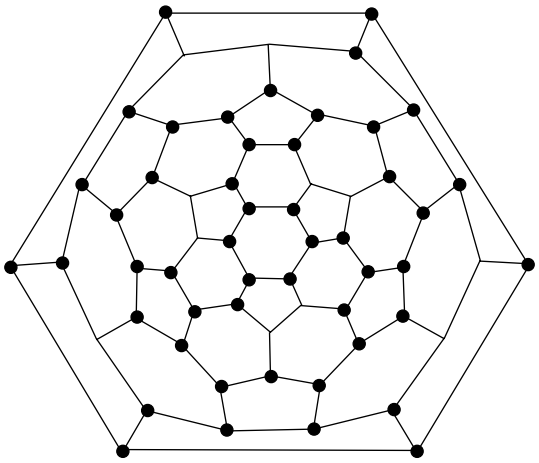

Fig. 1. Schlegel diagram for a $C_{60}F_{48}$ molecule. Circles denote fluorinated carbon atoms.

tion carbon–carbon double bonds, for example, by fluorination. At present, of all the known derivatives of the C_{60} fullerene, the $C_{60}F_{48}$ compound is the most fluorinated [14]. The electronic structure of $C_{60}F_{48}$ has been studied experimentally by photoelectron spectroscopy [14] and theoretically by the *ab initio* 6-31G method [15].

2. ATOMIC AND ELECTRONIC STRUCTURES OF $C_{60}F_{48}$ AND DETAILS OF THE CALCULATIONS

A $C_{60}F_{48}$ molecule has S_6 symmetry (the Schlegel diagram for a $C_{60}F_{48}$ molecule is shown in Fig. 1) [14]. There are three types of carbon hexagons in its atomic skeleton: two hexagons with six fluorine atoms each, twelve hexagons with five fluorine atoms each, and six hexagons with four fluorine atoms each. There are also two types of carbon pentagons: with five fluorine atoms (six pentagons) and with three fluorine atoms (six pentagons). Single carbon–carbon bonds are divided into four types (as shown by calculations using the *ab initio* 6-31G* method): 1.49, 1.54, 1.56, and 1.59 Å. The length of six double carbon–carbon bonds is 1.31 Å and the length of a fluorine–carbon bond is 1.34 Å.

The mechanisms of the interaction of low-energy protons (2–7 eV) with aromatic C_6H_6 and C_{60} molecules (carbon nanostructures (CNS)) and with their fluorine derivatives C_6F_{12} and $C_{60}F_{48}$ (fluorinated carbon nanostructures (FCNS)) were investigated using the methods of quantum chemistry and molecular dynamics. To better understand the role of the π system in the mechanism of inelastic proton scattering, we studied the potential barriers to the penetration of a helium atom through the carbon skeleton of CNS and FCNS.

The atomic and electronic structures of the above molecules with protons and helium atoms at different positions were calculated by the semiempirical PM3 method and the nonempirical *ab initio* 6-31G* method in the approximation of the unrestricted Hartree–Fock method (UHF) using the Gaussian code [16]. The optimization of the geometry was performed by the method of analytical gradient of the total electron energy. All potential barriers were calculated with allowance for the basic-set superposition error (BSSE). The potential curves for the interaction of a proton with optimized CNS and FCNS were calculated as functions of the distance between the proton and the center of the carbon hexagon lying strictly normal to the direction of motion of the H^+ ion. The penetration of low-energy protons through carbon hexagons and pentagons was simulated by the method of molecular dynamics using the UHF PM3 (MD/PM3) and *ab initio* 6-31G* (MD/6-31G*) potentials.

The applicability of one-determinant wave functions to the description of the electronic structure of fullerenes and their derivatives was confirmed earlier in [17]. An analysis of the UHF wave function for different proton positions with respect to the carbon skeleton of $C_{60}F_{48}$ has shown that the spin contamination to the wave function vanishes in a wide range of distances (0–5 Å). At chemically significant distances from the proton to the center of the carbon hexagon (from 0 to 6 Å), the energy difference between the HOMO and LUMO levels of the C_{60} + proton, $C_{60}F_{48}$ + proton, C_6H_6 + proton, and C_6F_{12} + proton systems varied from 5 to 8 eV (depending on the method, system, and distance); this might also argue for the applicability of one-determinant wave functions to the description of such processes. It should be specially noted that, because of the presence of a noncompensated positive charge in the systems under study, the occupied valence electron levels are displaced to lower energies to a much greater degree than the unoccupied levels and the number of electrons is always even (according to the condition of the problem). Calculations show that, in all cases, the electronic states are actually doubly occupied (because the orbitals with spin up and spin down in the UHF method have close energies and have the same character of spatial distribution) and, therefore, the electronic shells are closed.

The unrestricted Hartree–Fock method was chosen for the description of the electronic structure of such dynamic systems with a proton because the restricted Hartree–Fock method (RHF, or ROHF in the case of open electronic shells) and various versions of the DFT method incorrectly describe the self-interaction of an electron in the hydrogen 1*s* orbit (in these methods, the hydrogen 1*s* eigenvalues are ~6–8 eV, whereas the experimental value of the ionization potential and the UHF-calculated value are equal to approximately –13.5 eV; Table 1). This feature of the RHF and DFT methods does not make it possible to correctly describe the initial (at infinity) electronic state of the systems C_6F_{12} + proton and $C_{60}F_{48}$ + proton, which is formally excited: the hydrogen 1*s* state with an energy of about –13.5 eV

is unoccupied, and the HOMO level in CNS/FCNS with an energy higher than –12 eV is occupied. The results from calculating both the atomic and electronic structures of the systems under study agree well with the experimental data from [18].

The initial state of the "carbon nanostructure plus proton" system (proton–target molecule distance $R_H = -\infty$) is unstable and excited: the low-energy proton at infinity and the neutral molecule as a target (Fig. 2). Due to the substantial energy difference (6 eV for the proton + CNS system and 1.3 eV for the proton + FCNS system; Table 1), an electron transition should occur from the occupied electronic states of the carbon nanoparticle to the unoccupied 1*s* state of the positive hydrogen ion (which is essentially a proton) as the proton approaches the carbon nanostructure sufficiently closely (Fig. 2). For the systems H^+ + CNS and H^+ + FCNS (with the proton moving along the *Z* axis to the center of the carbon hexagon bonded to six fluorine atoms and oriented normal to the direction of the proton motion), we can write (in the first order of perturbation theory)

$$H = H_0^{\mathrm{H}} + H_0^{CN} + V_e(\mathbf{R}_{\mathrm{H}}) - \frac{\nabla_p^2(\mathbf{R}_{\mathrm{H}})}{2m_p} + V_N(\mathbf{R}_{\mathrm{H}}). \quad (1)$$

Here, H_0^{H} and H_0^{CN} are the Hamiltonians of the unperturbed electronic systems of the proton (having an unoccupied 1*s* orbit) and of the carbon nanostructure and $\mathbf{R}_{\mathrm{H}}$ is the radius vector of the proton, which is parallel to the proton velocity and whose length $|\mathbf{R}_{\mathrm{H}}| = t\sqrt{2E_K^p/m_p}$ is equal to the distance between the proton and the center of the carbon hexagon distance. The time *t* changes from $-\infty$ to 0; $-\nabla_p^2(\mathbf{R}_{\mathrm{H}})/(2m_p)$ is the operator of the proton kinetic energy; E_K^p is the proton kinetic energy (~10 eV in our case); and $V_e(\mathbf{R}_{\mathrm{H}})$ and $V_N(\mathbf{R}_{\mathrm{H}})$ are the operators of the Coulomb perturbation for the electronic and nuclear subsystems, respectively, describing the interaction of the uncompensated charge of the proton (H^+) with the Mulliken charges of the atoms of CNS or FCNS.

Modern nonempirical molecular dynamics [19] describes the motion of nuclei only for potential surfaces satisfying the Born–Oppenheimer approximation, for which one can write the relation $\sqrt{2E_K^p/m_p} \ll \sqrt{2E_K^e/m_e}$, where E_K^e is the electron kinetic energy and m_p and m_e are the proton and electron masses, respectively. With regard for the relation between the masses $m_p/m_e \cong 2 \times 10^3$ and the average kinetic energy of the valence electrons (E_K^e ~ 1–10 eV), this approximation can be applied to the description of the interaction of low-energy protons with matter if the proton kinetic energy is no less than $E_K^p \sim 10^2$–10^3 eV. In our case, $E_K^p \le 10$ eV.

Table 1. Theoretical (calculated under the approximation of the Coopmans theorem) and experimental ionization potentials of H, C_{60}, and $C_{60}F_{48}$ (in electronvolts)

Object	UHF PM3	*Ab initio* UHF/6-31G*	Experiment
H	13.1	13.6	13.6
C_{60}	9.5	7.6	7.6 [18]
$C_{60}F_{48}$	14.2	13.8	12.3 [14]

In the case where the kinetic energy is below this limit, we can separate the electronic and nuclear parts of Eq. (1). For the electronic part, in the first order of perturbation theory, we can write

$$\varepsilon'_{\mathrm{H}}(\mathbf{R}_{\mathrm{H}}) = \varepsilon^0_{\mathrm{H}} + \Delta\varepsilon_{\mathrm{H}}(\mathbf{R}_{\mathrm{H}}), \quad (2)$$

$$\varepsilon'_{CN}(\mathbf{R}_{\mathrm{H}}) = \varepsilon^0_{CN} + \Delta\varepsilon_{CN}(\mathbf{R}_{\mathrm{H}}), \quad (3)$$

where $\varepsilon'_{\mathrm{H}}(\mathbf{R}_{\mathrm{H}})$ and $\varepsilon'_{CN}(\mathbf{R}_{\mathrm{H}})$ are the excited electron energy eigenvalues corresponding to the unperturbed value $\varepsilon^0_{\mathrm{H}}$ (the energy of an unoccupied hydrogen 1*s* level) and to the unperturbed value ε^0_{CN} (the HOMO level of CNS/FCNS) localized on the proton and on the carbon nanocluster, respectively. For C_{60} and $C_{60}F_{48}$, we have $\varepsilon^0_{CN} = -7.6$ and –12.3 eV, respectively (the experimental values can be found in [18] and [14]; see Table 1).

Qualitatively, we can interpret the interaction of a low-energy proton with carbon (fluorine–carbon) nanoclusters in terms of perturbation theory. Disregarding the effects of orbital overlap, we can write the perturbation operator of the electronic system as

$$V_e(\mathbf{R}_{\mathrm{H}}) = V^{\mathrm{H}}(\mathbf{r}_{\mathrm{H}}) + V^{\mathrm{C}}(\mathbf{r}_{\mathrm{C}}) + V^{\mathrm{F}}(\mathbf{r}_{\mathrm{F}}), \quad (4)$$

where $\mathbf{r}_{\mathrm{H}}$, $\mathbf{r}_{\mathrm{C}}$, and $\mathbf{r}_{\mathrm{F}}$ are the radius vectors of the electronic wave functions belonging to the hydrogen, carbon, and fluorine ions, respectively; $V^{\mathrm{H}}(\mathbf{r}_{\mathrm{H}}) = -\sum_i^{N_{\mathrm{C}}} \frac{q_{\mathrm{C}}}{|\mathbf{r}_{\mathrm{H}} - \mathbf{R}_{\mathrm{C}}^i|} + \sum_j^{N_{\mathrm{F}}} \frac{q_{\mathrm{F}}}{|\mathbf{r}_{\mathrm{H}} - \mathbf{R}_{\mathrm{F}}^j|}$ operates only on the $\mathbf{r}_{\mathrm{H}}$ coordinate of the electron wave function (N_{C} and N_{F} are the numbers of carbon and fluorine atoms in the system, respectively); $V^{\mathrm{C}}(\mathbf{r}_{\mathrm{C}}) = -\sum_{i=1}^{N_{\mathrm{C}}} \frac{1}{|\mathbf{r}_{\mathrm{C}}^i + \mathbf{R}_{\mathrm{C}}^i|}$ operates on the $\mathbf{r}_{\mathrm{C}}$ coordinate; and $V^{\mathrm{F}}(\mathbf{r}_{\mathrm{F}}) = -\sum_{j=1}^{N_{\mathrm{F}}} \frac{1}{|\mathbf{r}_{\mathrm{F}}^j + \mathbf{R}_{\mathrm{F}}^j|}$ operates on the $\mathbf{r}_{\mathrm{F}}$ coordinate. The vectors $\mathbf{R}_{\mathrm{C}}^i$ and $\mathbf{R}_{\mathrm{F}}^j$

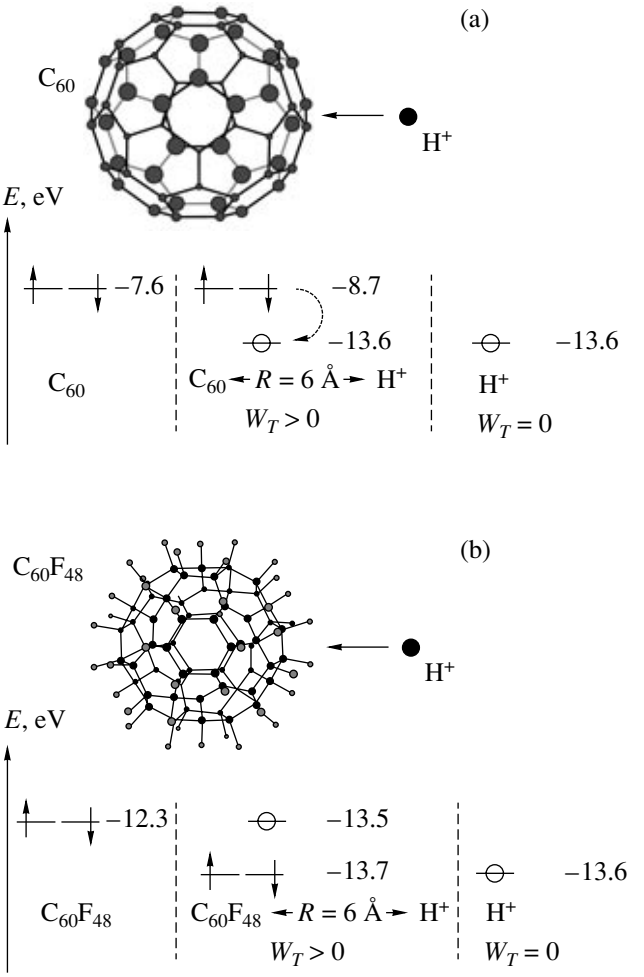

Fig. 2. Schematic representation of the interaction of a low-energy proton with (a) C_{60} and (b) $C_{60}F_{48}$ molecules. On the right, the unperturbed eigenvalue ε_H^0 of the hydrogen 1*s* orbital and, on the left, the unperturbed eigenvalue ε_{CN}^0 of the carbon nanoparticle are shown. At the center, perturbed eigenvalues ε'_{CN} and ε'_H are shown. W_T is the probability of charge transfer from the carbon nanoparticle to the proton. Over the distance range 0–6 Å in the case of C_{60} molecules, W_T varies from 0 to 1. In the latter case, the C_{60} molecule becomes a cation radical with the singly occupied $\varphi'_{CN}(\mathbf{r}_{CN})$ state and the proton becomes a hydrogen atom with the singly occupied $\varphi'_H(\mathbf{r}_H)$ state. In the case of the $C_{60}F_{48}$ molecule, charge transfer is suppressed due to the condition $\varepsilon'_{CN} < \varepsilon'_H$.

are directed from the proton to the carbon and fluorine atoms, respectively, and their lengths (for the nearest six neighbors) are $|\mathbf{R}_C^i| = \sqrt{R_H^2 + A^2}$ and $|\mathbf{R}_H^j| = \sqrt{(R_H - B)^2 + C^2}$. The geometrical parameters A = 1.4 Å, B = 1.1 Å, and C = 2.4 Å are determined by the features of the atomic structure of the object; q_C and q_F are the Mulliken charges of the carbon atoms (q_C is zero for C_6H_6 and C_{60} and is equal to ~0.1 for C_6F_{12} and $C_{60}F_{48}$) and fluorine atoms ($q_F \sim -0.1$).

The interaction $V_N(\mathbf{R}_H)$ between the uncompensated proton charge and the Mulliken charges of the atoms of the target molecule also contributes to the energy of the system. For nonfluorinated structures, we have $V_N(\mathbf{R}_H) = 0$, since the carbon Mulliken charges are zero. For fluorinated molecules ($C_{60}F_{48}$, C_6F_{12}), the quantity $V_N(\mathbf{R}_H) = \sum_i^{N_C} \frac{q_C}{|\mathbf{R}_C^i|} - \sum_j^{N_F} \frac{q_F}{|\mathbf{R}_F^j|}$ describes the contribution to the energy due to the interaction of the Mulliken charges of the carbon and fluorine atoms with the uncompensated proton charge.

The electronic structure of the system in the initial state of the process (neutral target molecule + proton at infinity) is quasi-excited (the energy of the unoccupied H1*s* state is –13.6 eV, and the energy of the HOMO level of the target molecule is higher than –12 eV; Table 1). As the proton approaches the target molecule, this excited state must decay with the emission of a photon and charge transfer via the electron transition from the target molecule to the proton or with the generation of molecular vibrations. The probability of one-electron dipole transition from the occupied orbital $\varphi_{CN}(\mathbf{r}_{CN})$ localized in the CNS/FCNS to the $\varphi_H(\mathbf{r}_H)$ orbital (the unoccupied hydrogen 1*s* orbital) can be written as [20]

$$w_T = 2|L_T|^2/(\hbar\omega)^2, \quad (5)$$

where $L_T = \langle \varphi'_{CN}(\mathbf{r}_{CN})|\mathbf{r}|\varphi'_H(\mathbf{r}_H)\rangle$, $\mathbf{r}$ is the dipole transition operator, and the transition energy is $\hbar\omega = \varepsilon'_{CN}(\mathbf{R}_H) - \varepsilon'_H(\mathbf{R}_H)$.The matrix element $L_T \neq 0$ if the overlap integrals for this system $S_{H-CN} = \langle \varphi_H|\varphi_{CN}\rangle \neq 0$ and $|\mathbf{R}_H| > 0$ (this condition is satisfied if the system has no mirror symmetry; this is the case for a substantial (of about 1 a.u.) separation between the proton and the center of the carbon hexagon). At large distances R_H (Fig. 2), the overlap integrals vanish. Our *ab initio* UHF/6-31G* calculations show that, starting from a distance of ~6 Å from the center of the carbon hexagon ($R_C < 6.3$ Å, $R_F < 5.8$ Å), the overlap integrals vary from 0 to 0.5. In this interval, $r(R_{CN})$ is equal to several angstroms; therefore, $w_T \approx S_{H-CN}$. The results obtained by the PM3 method show that, in the case of $C_{60}F_{48}$, at a distance of 6 Å, we have $\Delta\varepsilon_H$ = 0.1 eV and $\Delta\varepsilon_{CN}$ = –1.4 eV (ε'_H = –13.5 eV, ε'_{CN} = –13.7 eV). Thus, at distances of ≤6 Å, the $C_{60}F_{48}$ + proton configuration becomes the ground state of the system and the fluorinated carbon nanostructure interacts with a proton as does a neutral molecule with a point charge.

For a low-energy proton (~2 eV), the transit time for a distance of 6 Å is $T = 5 \times 10^{-14}$ s (for the C_{60} + proton system with $R_H < 6$ Å, the number of periods of the

electronic transition from the occupied state $\varphi_{CN}(\mathbf{r}_{CN})$ to the unoccupied state $\varphi_H(\mathbf{r}_H)$ (Fig. 2) is 10^2–10^3). For C_{60}, we have $\Delta\varepsilon_H = 0$ (the Mulliken charge of carbon atoms is zero) and $\Delta\varepsilon_{CN} = -1.15$ eV ($\varepsilon'_H = -13.6$ eV, $\varepsilon'_{CN} = -8.7$ eV). In this case, the transition frequency ω is 10^{16} s^{-1}; therefore, the total transition probability from the molecular level to the unoccupied H1*s* state (with regard for the number of periods of the electronic transition) is close to unity. The lifetime of the excited electronic state ($\tau \sim 5 \times 10^{-15}$–$3 \times 10^{-15}$ s) can be estimated from the experimental width of the photoelectron spectra (0.2–0.3 eV for C_{60} [21, 22] and $C_{60}F_{48}$ [14]; Fig. 3). This lifetime is an order of magnitude shorter than the proton transit time of the distance of 6 Å at which the overlap integral between the wave functions of the carbon nanoparticle and the proton becomes nonzero. Based on these estimations, we may assert that the aromatic molecules (C_{60}, C_6H_6) interact with a low-energy proton as do positive ion radicals (C_{60}^+, $C_6H_6^+$) with a radical (neutral hydrogen atom). This will certainly facilitate the formation of a new covalent carbon–hydrogen bond on the external side of the carbon nanoparticle.

Both theoretical quantum-chemical methods (UHF PM3 and *ab initio* UHF/6-31G*) correctly describe the initial FCNS + proton state, since the first ionization potential of $C_{60}F_{48}$ is overestimated (Table 1) and, therefore, the H1*s* state in the $C_{60}F_{48}$ + proton system remains unoccupied and all $C_{60}F_{48}$ levels are occupied. This feature allowed us to perform molecular-dynamics simulation of the interaction of protons with FCNS (C_6F_{12} and $C_{60}F_{48}$) using both the semiempirical and nonempirical quantum-chemical potentials. For comparison, we performed a molecular-dynamics simulation of the interaction of protons with aromatic carbon molecules (C_{60}, C_6H_6) with one difference: to avoid an error in describing the initial state (neutral molecule + proton at infinity), the initial distance between the proton and the carbon nanoparticle was chosen to be 2 Å. Thus, we assumed that, at this distance, the electron from the carbon nanoparticle has already passed to the proton with the formation of a hydrogen atom. We used the MD/PM3 and MD/UHF 6-31G* methods to simulate the interaction of a proton with C_6H_6 and C_6F_{12} and only the MD/PM3 method to simulate the interaction with C_{60} and $C_{60}F_{48}$ molecules.

To check the correctness of the calculations of the electronic structure by both methods, we compared the theoretical density of electronic states obtained using the UHF PM3 and *ab initio* UHF/6-31G[2] methods with the experimental photoelectron spectrum of $C_{60}F_{48}$ molecules [14] (Fig. 3) (results from comparisons of the theoretical and experimental spectra of other investigated molecules (C_6H_6, C_6F_{12}, C_{60}) can be easily found in the literature). We see that the theoretical calculations reproduce well the experimental data.

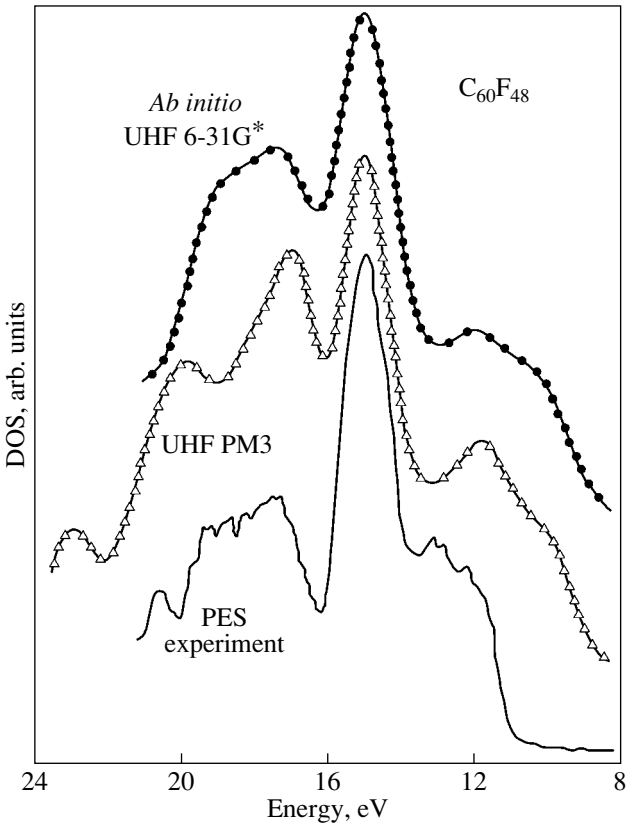

Fig. 3. Experimental photoelectron spectrum (solid line) [14] and the results of the *ab initio* UHF/6-31G* (circles) and UHF PM3 (triangles) calculations for the total density of states of the $C_{60}F_{48}$ molecule.

3. DISCUSSION

The potential curves for the interaction of a proton with $C_{60}F_{48}$ and C_{60} molecules calculated by the UHF PM3 and *ab initio* UHF/6-31G* methods are shown in Fig. 4. The distance R_H was measured from the proton to the center of the carbon hexagon (completely fluorinated in the case of $C_{60}F_{48}$) lying on the trajectory of the moving proton. The solid line shows the results obtained by the *ab initio* UHF/6-31G* method, and the dotted line corresponds to the UHF PM3 method. The closed triangle (the *ab initio* UHF/6-31G* method) and the open triangle (the UHF PM3 method) at infinity ($R = -\infty$) denote the total energy of the system in the initial state (neutral $C_{60}F_{48}$ and C_{60} molecules). Closed (the *ab initio* UHF/6-31G* method) and open (UHF PM3 method) squares denote the total energy of the system of the optimized $H–C_{60}F_{48}^+$ complex (with the hydrogen placed at the center of the carbon hexagon, $R = 0$, and the hydrogen covalently bonded to an sp^2 carbon inside the carbon polyhedron, $R = 5$ Å) and the

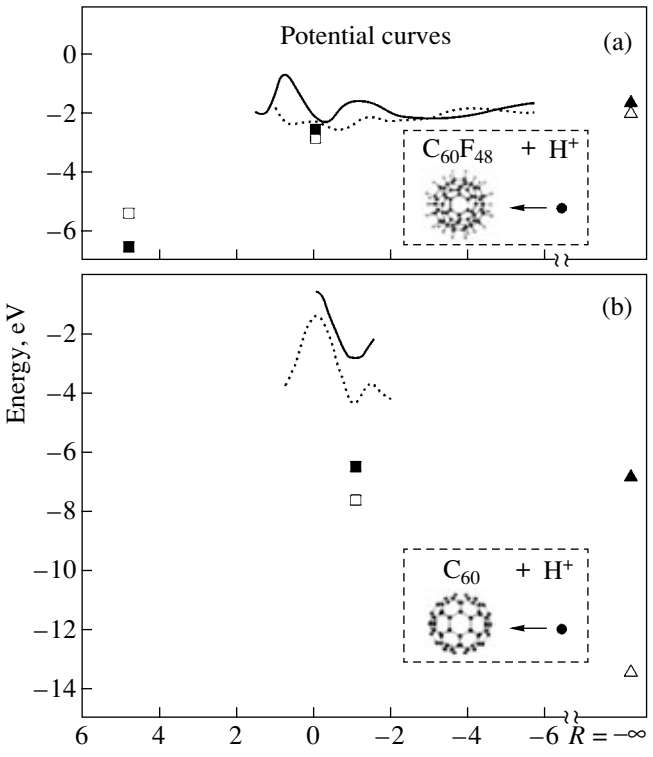

Fig. 4. Potential curves for the (a) $C_{60}F_{48} + H^+$ and (b) $C_{60} + H^+$ systems. Solid lines correspond to *ab initio* UHF/6-31G* calculations, and the dotted line, to UHF PM3 calculations. Closed triangles (*ab initio* UHF/6-31G*) and open triangles (UHF PM3) at a distance $R = -\infty$ denote the total energies of the (a) $C_{60}F_{48}$ and (b) C_{60} molecules. Closed (*ab initio* UHF/6-31G*) and open (UHF PM3) squares are the total energies of (a) the optimized $H–C_{60}F_{48}^+$ structures [with a hydrogen at the center of the carbon hexagon (R = 0) or with a covalently bonded hydrogen inside the carbon polyhedron (R = 5 Å)] and (b) the $H–C_{60}^+$ complex [with a covalently bonded hydrogen on the external side of the C_{60} molecule (R = –1 Å)].

$H–C_{60}^+$ complex (with the hydrogen covalently bonded to an sp^2 carbon outside the C_{60} molecule, R = –1 Å).

For the $C_{60}F_{48} + H^+$ system, the potential curves are typically smooth and do not exhibit high potential barriers or wells outside the carbon nanostructure or at the wall, whereas for the $C_{60} + H^+$ system two deep potential wells outside the carbon nanostructure, corresponding to the initial state (a neutral C_{60} molecule, $R = -\infty$) and to the hydrogen covalently bonded to a carbon atom (R = –1 Å), and one high potential barrier at the center of the carbon hexagon (R = 0). For the $C_{60}F_{48} + H^+$ system, a deep potential well exists inside the carbon polyhedron (R = 5 Å), corresponding to the hydrogen covalently bonded to an sp^2 carbon atom. This bond forms when the incident proton passes through the center of the carbon hexagon and collides with a nonfluorinated carbon atom located on the opposite side of the molecule.

The potential barriers to the penetration of the proton were calculated as the difference between the energies of the intermediate state (a guest atom at the center of the carbon hexagon) and of the initial state (the proton covalently bonded to a carbon atom on the external side of the carbon polyhedron [9]) or as the difference between the energies of the intermediate state and of the state of a neutral C_{60} molecule. The choice of the former initial state of the process of proton penetration through the carbon polyhedron is related not only to the desire to compare our data with those from [9] but also to the obvious fact that this configuration corresponds to the global energy minimum of the system, to which the system will tend in the case where the proton kinetic energy is close to zero. When studying the process of incorporation of a helium atom, the initial state was a $C_{60}/C_{60}F_{48}$ complex and a He atom at infinity.

Using the method of molecular dynamics, we calculated the kinetic energy of the penetration of a proton as the minimum kinetic energy required for the proton to penetrate into the molecule through the center of the carbon hexagon. In the case of the $C_{60}F_{48}$ molecule, the center of the completely fluorinated carbon hexagon was chosen as a target. The calculated penetration barriers are listed in Tables 2 and 3 (for the *ab initio* UHF/6-31G* and UFH PM3 methods, respectively).

The *ab initio* UHF/6-31G* calculations (Table 2) show a significantly lower barrier (by up to four times in the case of C_6H_6 and C_6F_{12} molecules) for the penetration of a proton through the carbon hexagon of fluorinated nanostructures (C_6F_{12} and $C_{60}F_{48}$) as compared to the barriers of nonfluorinated C_{60} and C_6H_6 molecules. We explain this result in terms of a substantial decrease in the density of valent π electrons on fluorinated nanoobjects, which precludes the formation of new covalent hydrogen–carbon bonds on the external side of the carbon polyhedron. Nevertheless, the potential barrier to the escape of the proton from the $C_{60}F_{48}$ molecule remains high (~5 eV) because of the formation of a new carbon–hydrogen covalent bond inside the carbon nanostructure (Fig. 4).

The potential barrier for a helium atom is 25% lower for fluorinated nanostructures as compared to nonfluorinated nanostructures (Table 2); this fact can be explained by the 12.5% lengthening of the carbon–carbon distance in a $C_{60}F_{48}$ molecule (1.59 Å) as compared to that in a C_{60} molecule (1.40 Å) and by the decrease in the density of π clouds at the center of the carbon hexagon.

For C_6H_6 and C_6F_{12} molecules, we performed the molecular-dynamics simulation using the *ab initio* UHF/6-31G* potential (MD/6-31G*). The proton kinetic energy at which the proton penetrates through the C_6 fragment turned out to be 2.6 times lower for a C_6F_{12} molecule (2.6 eV) than that for a benzene mole-

cule (6.7 eV; Table 2). We did not study the potential curves for the interaction of a proton with a C_6F_{12} molecule because of the substantial distortion of the C_6 fragment in this case and the impossibility of defining its center uniquely.

Similar results for the $C_6H_6 + H^+$ and $C_6F_{12} + H^+$ systems were also obtained by the semiempirical PM3 method (Table 3). The potential barrier for a $C_{60}F_{48}$ molecule (1.8 eV) turned out to be 3.6 times lower than that for a C_{60} molecule (6.5 eV). This ratio for the pair C_6F_{12} (4.8 eV) and C_6H_6 (6.5 eV) is much lower (~1.4), since the PM3 method predicts that the C–C bond in the C_6F_{12} molecule is broken by the proton. Simulation of the $C_{60} + H^+/C_{60}F_{48} + H^+$ and $C_6H_6 + H^+/C_6F_{12} + H^+$ processes using the MD/PM3 method showed that fluorination lowers the penetration barriers by factors of 4.1 and 1.5, respectively. It should be noted that, after the penetration into the carbon polyhedron of the $C_{60}F_{48}$ molecule, the proton forms a new C–H bond with an sp^2 carbon atom inside the carbon skeleton. Subsequent collisions with protons form either new carbon–hydrogen bonds inside the $C_{60}F_{48}$ molecule or H_2 molecules via the breaking of the earlier formed carbon–hydrogen bonds.

We also studied other channels of inelastic scattering of protons by a $C_{60}F_{48}$ molecule using the MD/PM3 method. For a target, we chose (i) a carbon atom not bonded to a fluorine atom, (ii) the center of the double carbon–carbon bond, (iii) the center of the carbon pentagon, (iv) a fluorine atom, (v) the center of the carbon–fluorine bond, and (vi) a series of points on an imaginary surface of carbon pentagons and hexagons lying far from their centers.

Molecular-dynamics simulation showed that there are several channels of inelastic scattering of protons with a kinetic energy of about 2 eV.

(1) Breaking of a C–F bond with the formation of an HF molecule (collisions with a carbon atom, with the centers of the carbon–carbon and carbon–fluorine bonds).

(2) Penetration into a $C_{60}F_{48}$ molecule (through a series of points on the imaginary surface of carbon pentagons and hexagons).

(3) Reflection of the proton with partial absorption of its kinetic energy via the excitation of molecular vibrations of the $C_{60}F_{48}$ molecule (in particular, due to collisions with fluorine atoms).

The results of the MD/PM3 calculations showed that, on the imaginary surface of carbon hexagons in $C_{60}F_{48}$, there are regions with a reduced electronic density that are open for proton penetration. For example, for a kinetic energy of 2 eV, the diameter of such a region is ~1.5 Å. Therefore, approximately 25% of the imaginary surface of the carbon polyhedron of fluorinated nanoobjects is open for proton penetration through the walls.

Table 2. Potential barriers and the kinetic energy required for a proton to penetrate through the center of a carbon hexagon (results of *ab initio* UHF/6-31G* calculations)

Object	Potential barrier, eV	Kinetic energy, eV
$C_6H_6 + H^+$	5.6	6.7
$C_6F_{12} + H^+$	1.4	2.6
$C_{60} + H^+$	6.2 (6.3)	–
$C_{60}F_{48} + H^+$	3.1	–
$C_{60} + He$	14.0	–
$C_{60}F_{48} + He$	10.5	–

Note: The potential barrier calculated as the difference between the energies of the intermediate state (with a proton at the center of the hexagon) and of the free C_{60} molecule is indicated in parentheses. The calculations were performed with regard for the superposition error.

Table 3. Potential barriers and the kinetic energy required for a proton to penetrate through carbon hexagons (the results of the UHF PM3 calculations)

Object	Potential barrier, eV	Kinetic energy, eV
$C_6H_6 + H^+$	6.5	5.6
$C_6F_{12} + H^+$	4.8	3.7
$C_{60} + H^+$	6.5 (12.0*)	5.7
$C_{60}F_{48} + H^+$	1.8	1.4

* The meaning of the parenthetical value is explained in the note to Table 2.

4. CONCLUSIONS

In this study, we have shown that, starting from a distance of ~6 Å, the electronic charge transfer determines the character of interaction of low-energy protons with aromatic molecules and transforms a proton into a hydrogen atom and a neutral target molecule into a cation radical. In turn, this circumstance facilitates the formation of a new covalent carbon–hydrogen bond outside the carbon nanoparticle and determines the nature of the potential barrier to the penetration of a proton through carbon pentagons and hexagons.

The presence of substitutional fluorine atoms suppresses the electronic charge transfer from C_6F_{12} and $C_{60}F_{48}$ due to the Coulomb perturbation of the electronic structure of an interacting system. In this case, the neutral $C_6F_{12}/C_{60}F_{48}$ molecule + proton state becomes the ground state and, therefore, the low-energy proton interacts with fluorinated carbon nanoparticles as a point charge does with a neutral molecule. At short (chemically significant) distances of ~2 Å, the absence of the π-electron density on the external side of the carbon polyhedron precludes the formation of a new C–H bond. In turn, this lowers the barriers to the penetration of low-energy protons through the carbon core by a factor of 2–4.

Molecular-dynamics calculations using the nonempirical 6-31G* and semiempirical potentials have shown that, for a proton kinetic energy of 2 eV, a quarter of the imaginary surface of the carbon core of the fluorine-substituted carbon molecules is open for the penetration of low-energy protons. However, the barrier to the escape of a proton from such molecules remains high because of the formation of new covalent carbon–hydrogen bonds inside the systems under study. Other scattering channels result either in the carbon–fluorine bond breaking (with the formation of HF molecules) or in the reflection of a proton from the molecules with a loss of part of the kinetic energy due to the excitation of molecular vibrations in the fluorine–carbon nanoparticle.

ACKNOWLEDGMENTS

This study was supported by the Nanoscale Science and Engineering Initiative of the National Science Foundation, grant no. EEC-0118007 (Rice CBEN), and by the Welch Foundation.

REFERENCES

1. J. R. Heath, S. C. O'Brien, Q. Zhang, Y. Liu, R. F. Curl, H. W. Kroto, F. K. Tittel, and R. E. Smalley, J. Am. Chem. Soc. **107**, 7779 (1985).
2. Y. Chai, T. Guo, C. Jin, R. E. Haufler, L. P. F. Chibante, J. Fure, L. Wang, J. M. Alford, and R. E. Smalley, J. Phys. Chem. **95**, 7564 (1991).
3. M. Saunders, H. A. Jimenez-Vazquez, R. J. Cross, and R. J. Poreda, Science (Washington) **259**, 1428 (1993); F. Hensel and P. Edwards, Science (Washington) **271**, 1693 (1996).
4. J. J. Christian, Z. Wan, and S. L. Anderson, Chem. Phys. Lett. **199**, 373-8 (1992).
5. T. A. Murphy, T. Pawlik, A. Weidinger, M. Höhne, R. Alcala, and J. M. Spaeth, Phys. Rev. Lett. **77**, 1075 (1996).
6. E. E. B. Campbell, R. Tellgmann, N. Krawez, and I. V. Hertel, J. Phys. Chem. Solids **58**, 1763 (1997).
7. T. Ohtsuki, K. Ohno, K. Shiga, Y. Kawazoe, Y. Maruyama, and K. Masumoto, Phys. Rev. Lett. **81**, 967 (1998).
8. D. S. Bethune, R. D. Johnson, J. R. Salem, M. S. de Vries, and C. M. Yannoni, Nature (London) **366**, 123 (1993).
9. S. K. Estreicher, C. D. Lathan, M. I. Heiggie, R. Jones, and S. Öberg, Chem. Phys. Lett. **196**, 311 (1992).
10. K. C. Mowrey, M. M. Ross, and J. H. Callahan, J. Phys. Chem. **96**, 4755 (1992).
11. M. Kolb and W. Thiel, J. Comput. Chem. **14**, 37 (1993).
12. J. Hru§ak, D. K. Böhme, T. Weiske, and H. Schwarz, Chem. Phys. Lett. **193**, 97 (1992).
13. K. Ohno, Y. Maruyama, K. Esfarjani, and Y. Kawazoe, Phys. Rev. Lett. **76**, 3590 (1996).
14. R. Mitsumoto, T. Araki, E. Ito, Y. Ouchi, K. Seki, K. Kikuchi, Y. Achiba, H. Kurosaki, T. Sonoda, H. Kobayashi, O. V. Boltalina, V. K. Pavlovich, L. N. Sidorov, Y. Hattori, N. Liu, S. Yajima, S. Kawasaki, F. Okino, and H. Touhara, J. Phys. Chem. A **102**, 552 (1998).
15. L. G. Bulusheva, A. V. Okotrub, and O. V. Boltalina, J. Phys. Chem. A **103**, 9921 (1999).
16. M. J. Frisch, G. W. Trucks, H. B. Schlegel, G. E. Scuseria, M. A. Robb, J. R. Cheeseman, V. G. Zakrzewski, J. J. A. Montgomery, K. N. Kudin, J. C. Burant, J. M. Millam, R. E. Stratmann, J. Tomasi, V. Barone, B. Mennucci, M. Cossi, G. Scalmani, N. Rega, S. Iyengar, G. A. Petersson, M. Ehara, K. Toyota, H. Nakatsuji, C. Adamo, J. Jaramillo, R. Cammi, C. Pomelli, J. Ochterski, P. Y. Ayala, K. Morokuma, P. Salvador, J. J. Dannenberg, S. Dapprich, A. D. Daniels, M. C. Strain, O. Farkas, D. K. Malick, A. D. Rabuck, K. Raghavachari, J. B. Foresman, J. V. Ortiz, Q. Cui, A. G. Baboul, S. Clifford, J. Cioslowski, B. B. Stefanov, G. Liu, A. Liashenko, P. Piskorz, I. Komaromi, R. Gomperts, R. L. Martin, D. J. Fox, T. Keith, M. A. Al-Laham, C. Y. Peng, A. Nanayakkara, M. Challacombe, P. M. W. Gill, B. Johnson, W. Chen, M. W. Wong, J. L. Andres, C. Gonzalez, M. Head-Gordon, E. S. Replogle, and J. A. Pople, *GAUSSIAN 01: Development Version (Revision B.01)* (Gaussian Inc., Pittsburgh, PA, 2001).
17. W. Andreoni, Annu. Rev. Phys. Chem. **49**, 405 (1998).
18. K. Hedberg, L. Hedberg, D. S. Bethune, C. A. Brown, M. S. de Vries, and R. D. Johnson, Science (Washington) **254**, 410 (1991).
19. R. Car and M. Parinello, Phys. Rev. Lett. **55** (22), 2471 (1985).
20. L. D. Landau and E. M. Lifshitz, *Course of Theoretical Physics*, Vol. 3: *Quantum Mechanics: Non-Relativistic Theory* (Nauka, Moscow, 1974; Pergamon, New York, 1977).
21. J. H. Weaver, Acc. Chem. Res. **25**, 143 (1992).
22. S. A. Varganov, P. V. Avramov, and S. G. Ovchinnikov, Fiz. Tverd. Tela (St. Petersburg) **42**, 2103 (2000) [Phys. Solid State **42**, 2168 (2000)].

Translated by I. Zvyagin